

Article ID: 1001-0742(2005)02-0290-04

CLC number: X505

Document code: A

# Enhanced photocatalytic activity of nanotube-like titania by sulfuric acid treatment

YANG Shao-gui, QUAN Xie\*, LI Xin-yong, FANG Ning, ZHANG Ning, ZHAO Hui-min

(School of Environmental and Biological Science and Technology, Dalian University of Technology, Dalian 116024, China. E-mail: quanxie@dlut.edu.cn)

**Abstract:** The TiO<sub>2</sub> nanotube sample was prepared via a NaOH solution in a Teflon vessel at 150 °C. The as-prepared nanotubes were then treated with H<sub>2</sub>SO<sub>4</sub> solutions. The TiO<sub>2</sub> nanotube has a crystalline structure with open-ended and multiwall morphologies. The TiO<sub>2</sub> nanotubes before and after surface acid treatment were characterized by X-ray diffraction (XRD), scanning electron microscopy (SEM), transmission electron microscopy (TEM) and UV-VIS dispersive energy spectrophotometry (DRS). The photocatalytic activity of the samples was evaluated by photocatalytic degradation of acid orange II in aqueous solutions. It was found that the order of photocatalytic activity was as follows: TiO<sub>2</sub> nanotubes treated with 1.0 mol/L H<sub>2</sub>SO<sub>4</sub> solution (TiO<sub>2(1.0M H<sub>2</sub>SO<sub>4</sub>)</sub> nanotubes) > TiO<sub>2</sub> nanotubes treated with 0.2 mol/L H<sub>2</sub>SO<sub>4</sub> solution (TiO<sub>2(0.2M H<sub>2</sub>SO<sub>4</sub>)</sub> nanotubes) > TiO<sub>2</sub> nanotubes > TiO<sub>2</sub> powder. This was attributed to the fact that TiO<sub>2</sub> nanotubes treated with H<sub>2</sub>SO<sub>4</sub> was composed of smaller particles and had higher specific surface areas. Furthermore, the smaller TiO<sub>2</sub> particles were beneficial to the transfer and separation of photo-generated electrons and holes in the inner of and on the surface of TiO<sub>2</sub> particles and reduced the recombination of photo-generated electrons and holes. Acid treatment was particularly effective for TiO<sub>2</sub> nanotubes, this increase in activity was correlated with the concentration of H<sub>2</sub>SO<sub>4</sub> solution.

**Keywords:** titania nanotube; photocatalytic activity; acid orange II; H<sub>2</sub>SO<sub>4</sub> solutions

## Introduction

TiO<sub>2</sub> nanotube has widely drawn much attention due to its large surface area and high photocatalytic activity, because they have great potential for such applications as environmental purification, decomposition of carbonic acid gas, and generation of hydrogen gas. Titania nanotubes of different geometrical shapes and microstructures in powdery forms have been fabricated by various research groups using techniques like sol-gel synthesis (Caruso, 2001; Hoyer, 1996; Kasuga, 1998), freeze-drying (Ma, 2003), electrodeposition (Zhang, 2002; Adachi, 2000), sonochemical deposition (Zhu, 2001), and methods involving the chemical treatment of fine titania particles (Imai, 1999; Kasuga, 1999; Du, 2001; Michailowski, 2001). Via a simple hydrothermal treatment of crystalline TiO<sub>2</sub> particles with NaOH solutions, Kasuga *et al.* (Kasuga, 1998; 1999) produced high quality TiO<sub>2</sub> nanotubes with uniform diameters of around 12 nm. Following their pioneering work, several research groups have also synthesized TiO<sub>2</sub> nanotubes by the similar chemical processes. While little report on photocatalytic activity of titania nanotube formed via the treatment of NaOH solutions was found. So in this work we prepared titania nanotube via alkali treatment and studied its photocatalytic activity towards acid orange II. Up to now, to our knowledge, we firstly presented the comparative studies of photocatalytic activity of TiO<sub>2</sub> nanotubes and TiO<sub>2</sub> nanotubes treated with H<sub>2</sub>SO<sub>4</sub> solutions. We found that the photocatalytic activity of TiO<sub>2</sub> nanotubes could be greatly improved by H<sub>2</sub>SO<sub>4</sub> solution treatment. Explanations are

provided based on the influence of surface microstructure of TiO<sub>2</sub> powder and surface acid treatment on photocatalytic activity.

## 1 Experimental

### 1.1 Materials

Tetrabutylorthotitanate, HCl, H<sub>2</sub>SO<sub>4</sub> acid and NaOH were used (analytical grade) and bought from Shenyang Chemical Company in P. R. China.

The acid orange II was obtained from the Fine Chemistry Key Laboratory of the State, Dalian University of Technology.

All compounds were used without further purification.

### 1.2 Preparation of TiO<sub>2</sub> nanotube by different method

The TiO<sub>2</sub> nanotube sample was synthesized by using a similar process to that reported by Kasuga *et al.* (Kasuga, 1998). TiO<sub>2</sub> powder (T1) were formed by the hydrolysis of tetrabutylorthotitanate and heat treatment at 500 °C for 1 h. Subsequently, further treatment with a NaOH (10 mol/L) solution in a Teflon vessel at 150 °C was carried out for 20 h. After being washed with a 0.1 mol/L HCl solution and deionized water, white color products were obtained and pH value was about 7.0. Then the sample was treated at 500 °C for 1 h and the TiO<sub>2</sub> nanotube sample was obtained.

### 1.3 Treatment of TiO<sub>2</sub> nanotube with sulfuric acid solutions

The calcined TiO<sub>2</sub> nanotube sample was exposed to 0.2 mol/L and 1.0 mol/L H<sub>2</sub>SO<sub>4</sub> for 30 min, respectively. The ratio of 1.0 g of titania nanotube to 15 ml of the sulfuric acid solutions was used. The resulting TiO<sub>2</sub>/H<sub>2</sub>SO<sub>4</sub> nanotube samples were washed by deionized water and dried at 110 °C,

and then calcined at elevated temperatures to obtain the final sulfated  $\text{TiO}_2$  nanotube samples (marked by  $\text{TiO}_{2(0.2\text{M H}_2\text{SO}_4)}$  and  $\text{TiO}_{2(1.0\text{M H}_2\text{SO}_4)}$  nanotubes, respectively).

#### 1.4 Characterization of titanium dioxide nanotube

SEM and TEM images were obtained with scanning electron microscope (JSM-5600LV) and a transmission electron microscope (Hitachi-600), respectively. The X-ray diffraction (XRD) patterns, obtained on a Philips MPD 18801 X-ray diffractometer using  $\text{Cu K}_\alpha$  radiation ( $\lambda = 0.15406 \text{ nm}$ ) at a scan rate of  $0.05 (2\theta)/\text{s}$ , were used to determine the identity of any phase present and their crystallite size. The accelerating voltage and the applied current are 40 kV and 30 mA, respectively. The crystallite size was calculated from X-ray line broadening analysis by Scherrer formula. UV-VIS dispersive energy spectra were obtained using a UV-VIS spectrophotometer (UV550, Jasco).

#### 1.5 Photocatalytic activity

Azo dyes are used in virtually every commercial coloration process. Acid orange II widely presented in the wastewater of dyes and caused a serious public health problem. Therefore, we chose it as a model contaminate chemical.

The columned photoreactor was made of glass and its diameter and height was 2 cm and 26 cm, respectively. The dye solution was illuminated by 300 W high pressure mercury lamp (Shanghai Yaming Lamp Factory, China) with a maximum centered at  $\lambda = 365 \text{ nm}$ . The UV-VIS spectrophotometer (UV-VIS 550, Jasco) was employed to determine the concentration and the pH value of the acid orange II solutions.

All experiments were operated at room temperature (around  $20^\circ\text{C}$ ). The concentration of acid orange II was 20 mg/L without special explanations. The decolorization efficiency was defined as:

$$\text{Decolorization efficiency}(\%) = \frac{C_0 - C}{C_0} \times 100\%, \quad (1)$$

in which  $C_0$  is the initial concentration (mg/L);  $C$  is the concentration at  $T$  time (mg/L).

## 2 Results and discussion

### 2.1 XRD analysis

X-ray diffraction experiments have been performed to compare the crystalline phase of the  $\text{TiO}_2$  nanotube samples. Fig. 1 shows the XRD profiles taken from  $\text{TiO}_2$  powder,  $\text{TiO}_2$  nanotubes,  $\text{TiO}_{2(0.2\text{M H}_2\text{SO}_4)}$  nanotubes and  $\text{TiO}_{2(1.0\text{M H}_2\text{SO}_4)}$  nanotubes, respectively. It is evident from Fig. 1 that the films prepared by the sol-gel procedure presented very good crystallization, which was nearly anatase form of titanium dioxide. The peaks at  $2\theta = 25.5^\circ$  in the spectrum of  $\text{TiO}_2$  are easily identified as the crystal of anatase phase. It is noted

that the peak (101) of  $\text{TiO}_{2(0.2\text{M H}_2\text{SO}_4)}$  and  $\text{TiO}_{2(1.0\text{M H}_2\text{SO}_4)}$  nanotubes was broaden compared with  $\text{TiO}_2$  powder and  $\text{TiO}_2$  nanotubes, which indicated that  $\text{TiO}_{2(0.2\text{M H}_2\text{SO}_4)}$  and  $\text{TiO}_{2(1.0\text{M H}_2\text{SO}_4)}$  nanotubes were composed of finer nanoparticle due to the acidification. Furthermore, the average crystalline sizes calculated using the diffraction peaks (101) from Scherrer's formula (Sene, 2003) of  $\text{TiO}_2$  powder,  $\text{TiO}_2$  nanotubes,  $\text{TiO}_{2(0.2\text{M H}_2\text{SO}_4)}$  nanotubes and  $\text{TiO}_{2(1.0\text{M H}_2\text{SO}_4)}$  nanotubes were in the range of 15, 14, 8 and 7 nm, respectively.

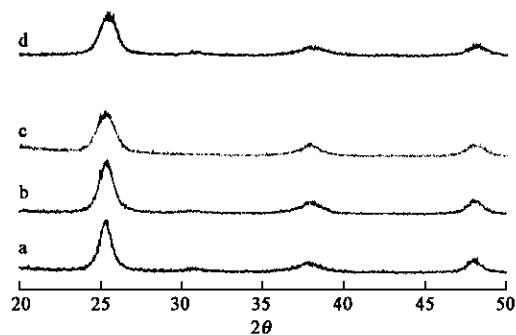


Fig. 1 XRD patterns of different  $\text{TiO}_2$  nanotubes acidified  
a.  $\text{TiO}_2$  powder; b.  $\text{TiO}_2$  nanotubes; c.  $\text{TiO}_{2(0.2 \text{ mol/L H}_2\text{SO}_4)}$  nanotubes; d.  $\text{TiO}_{2(1.0 \text{ mol/L H}_2\text{SO}_4)}$  nanotubes

### 2.2 SEM analysis

Fig. 2 is SEM images of  $\text{TiO}_2$  samples. It is obviously seen from Fig. 2A that  $\text{TiO}_2$  nano-particles were assembled in the  $\text{TiO}_2$  powder. As clearly seen in Fig. 2B and C, numerous fiberlike nanotubes grew from a micro-size  $\text{TiO}_2$  particles. These nanotubes in  $\text{TiO}_{2(0.2\text{M H}_2\text{SO}_4)}$  and  $\text{TiO}_{2(1.0\text{M H}_2\text{SO}_4)}$  samples had an outer diameter between 10 and 20 nm. They are about 12 nm in diameter, in line with the results reported in the literature (Kasuga, 1998; 1999; Du, 2001). A TEM image of  $\text{TiO}_2$  nanotube near its tube opening is presented in Fig. 3. The hollow nature of the nanotube is clearly visible in the TEM image. It indicated from Fig. 2B and Fig. 2C that the surface microstructure of  $\text{TiO}_2$  and  $\text{TiO}_{2(1.0\text{M H}_2\text{SO}_4)}$  nanotubes before and after surface acid treatment had no obvious changes, yet  $\text{TiO}_{2(1.0\text{M H}_2\text{SO}_4)}$  nanotubes seemed like more incompact than  $\text{TiO}_2$  nanotubes.

### 2.3 UV-visible dispersive reflectance spectra (DRS) analysis

The UV-VIS absorption spectra of  $\text{TiO}_2$  powder,  $\text{TiO}_2$  nanotubes and  $\text{TiO}_{2(0.2\text{M H}_2\text{SO}_4)}$  and  $\text{TiO}_{2(1.0\text{M H}_2\text{SO}_4)}$  nanotubes are shown in Fig. 4. For four samples, the absorption is about 0.9 at the range of wavelength from 200 nm to 310 nm. At longer wavelength, the absorption of  $\text{TiO}_2$  nanotubes decreases and approaches zero at about 400 nm, while at the 350 nm, the absorption of  $\text{TiO}_2$  powder,  $\text{TiO}_{2(0.2\text{M H}_2\text{SO}_4)}$  and

$\text{TiO}_2(1.0\text{M H}_2\text{SO}_4)$  nanotubes start to decrease and is close to zero at 400 nm. Comparing these four curves, the absorption edge of  $\text{TiO}_2$  nanotubes is observed at a shorter wavelength range than that of  $\text{TiO}_2$  powder,  $\text{TiO}_2(0.2\text{M H}_2\text{SO}_4)$  and  $\text{TiO}_2(1.0\text{M H}_2\text{SO}_4)$  nanotubes. The shift is considered to occur due to the difference in crystallites within the nanotube samples.  $\text{TiO}_2$

nanotubes consists of relatively small crystallites and showed a pseudo "blue shift" like fine particle (Anpo, 1987; Duonghong, 1981). The difference of absorption between  $\text{TiO}_2$  nanotubes and  $\text{TiO}_2$  powder was attributed to the difference in their absorption of light.

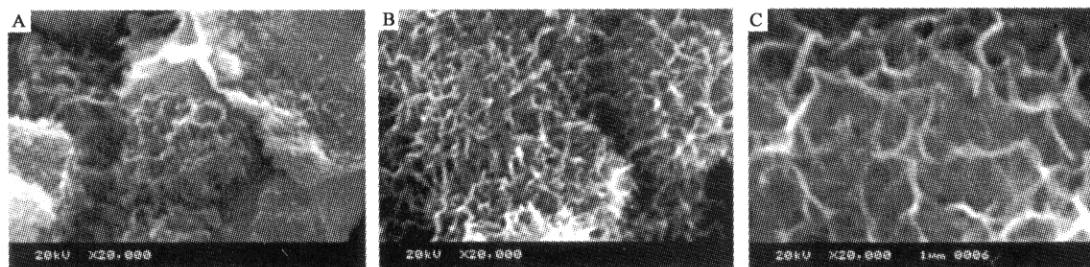


Fig. 2 SEM images of  $\text{TiO}_2$  powders(A);  $\text{TiO}_2$  nanotubes(B);  $\text{TiO}_2(1.0\text{ mol/L H}_2\text{SO}_4)$  nanotubes(C)

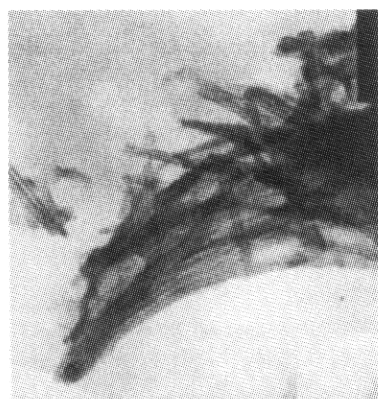


Fig. 3 TEM image of  $\text{TiO}_2$  nanotube formed via a NaOH solutions treatment at in a Teflon vessel at  $150^\circ\text{C}$  for 20 h

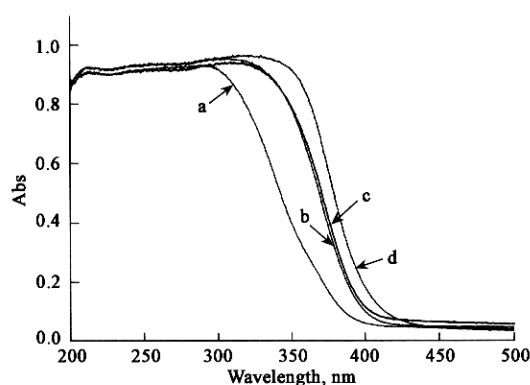


Fig. 4 UV-VIS dispersive reflectance spectra of  $\text{TiO}_2$  nanotubes (a);  $\text{TiO}_2(0.2\text{ M H}_2\text{SO}_4)$  nanotubes(b);  $\text{TiO}_2(1.0\text{ M H}_2\text{SO}_4)$  (c); and  $\text{TiO}_2$  powder(d)

It is seen clearly from Fig. 4 that the absorption ability of  $\text{TiO}_2$  nanotubes ( $< 400\text{ nm}$ ) was the best, that of  $\text{TiO}_2(0.2\text{M H}_2\text{SO}_4)$  and  $\text{TiO}_2(1.0\text{M H}_2\text{SO}_4)$  nanotubes was medium, and that of  $\text{TiO}_2$  powder was the worst. In other words, the band gap energy of  $\text{TiO}_2$  nanotubes is the highest, that of  $\text{TiO}_2(0.2\text{M H}_2\text{SO}_4)$  and  $\text{TiO}_2(1.0\text{M H}_2\text{SO}_4)$  was medium, and that of

$\text{TiO}_2$  powder was the lowest.

## 2.4 Photocatalytic activity

Photocatalytic degradation experiments of acid orange II were performed in a photocatalytic reactor mentioned above. The conditions of photocatalytic experiment were as follows: initial concentration of acid orange II was 20 mg/L, pH value of the solutions was about 7.2, the concentration of titania was 0.2 mg/L.

### 2.4.1 Comparative study of photocatalytic activity of $\text{TiO}_2$ powder and $\text{TiO}_2$ nanotubes

It can be seen from Fig. 5 that photocatalytic activity of  $\text{TiO}_2$  nanotubes is obviously higher than that of  $\text{TiO}_2$  powder. The degradation rate of acid orange II in  $\text{TiO}_2$  nanotubes photocatalyst is apparently faster than that of acid orange II in  $\text{TiO}_2$  powder. And decoloration efficiencies of target chemical in the presence of  $\text{TiO}_2$  nanotubes and  $\text{TiO}_2$  powder were 85% and 90% during 2 h reaction time, respectively. Characterization results of XRD, SEM and DRS can explain the enhancement in photocatalytic activity. Firstly, XRD results showed that  $\text{TiO}_2$  nanotubes possess smaller size and much larger surface area, which resulted in a higher photodegradation rate. Secondly, UV-VIS DRS showed that the absorption edge of  $\text{TiO}_2$  nanotubes is at a shorter wavelength range than that of  $\text{TiO}_2$  powder. This indicated crystallites in  $\text{TiO}_2$  powder with lightly higher band-gap energy and a stronger oxidation power (Linsebigler, 1995). All these factors can enhance the photocatalytic activity of  $\text{TiO}_2$  nanotubes prepared via NaOH solutions in a vessel at  $150^\circ\text{C}$ .

### 2.4.2 Effects of surface acid treatment on photocatalytic activity of $\text{TiO}_2$ nanotube

As shown in Fig. 6,  $\text{TiO}_2$  nanotubes and  $\text{TiO}_2(0.2\text{M H}_2\text{SO}_4)$  and  $\text{TiO}_2(1.0\text{M H}_2\text{SO}_4)$  nanotubes displayed the different photocatalytic activity towards acid orange II. The

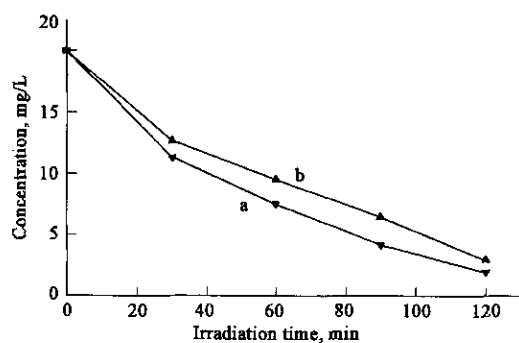


Fig. 5 Photocatalytic oxidation of acid orange II in the presence of  $\text{TiO}_2$  nanotubes formed via NaOH treatment(a) and  $\text{TiO}_2$  powder(b)

The concentration of addition of samples: 0.2 mg/L

photocatalytic activity of  $\text{TiO}_2$  nanotubes and  $\text{TiO}_{2(0.2\text{M H}_2\text{SO}_4)}$  and  $\text{TiO}_{2(1.0\text{M H}_2\text{SO}_4)}$  nanotubes follows the order:  $\text{TiO}_2$  nanotubes <  $\text{TiO}_{2(0.2\text{M H}_2\text{SO}_4)}$  nanotubes <  $\text{TiO}_{2(1.0\text{M H}_2\text{SO}_4)}$  nanotubes. This was attributed to the fact that  $\text{TiO}_{2(0.2\text{M H}_2\text{SO}_4)}$  and  $\text{TiO}_{2(1.0\text{M H}_2\text{SO}_4)}$  nanotubes were composed of smaller particles, because more breadth of the peak(101) were found in Fig. 1c and Fig. 1d and they had higher specific surface area. Furthermore, the monodispersity of  $\text{TiO}_2$  particles was beneficial to transfer and separate photo-generated electrons and holes in the inner of and on the surface of  $\text{TiO}_2$  particle and reduced the recombination of photo-generated electrons and holes. During 60 min reaction time the decoloration efficiencies of acid orange II in the presence of  $\text{TiO}_2$  nanotubes and  $\text{TiO}_{2(0.2\text{M H}_2\text{SO}_4)}$  and  $\text{TiO}_{2(1.0\text{M H}_2\text{SO}_4)}$  nanotubes were 62.5%, 79.7% and 92.2%, respectively.

Considering the acid orange II oxidation as a first-order decay process, mass balance results in

$$C_t = C_0 \exp(-kt) \quad (2)$$

Where  $C_0$  is the initial concentration,  $t$  is the treatment time, and  $k$  is the kinetic constant or the apparent rate constant for PCP oxidation. The slope in the plot of  $\ln[C_0/C_t]$  vs  $t$  leads to the kinetic constant. The kinetics constants and regression coefficient is shown in Table 1.

Table 1 Kinetic constants and relative coefficients of acid orange II in the presence of different photocatalysts

	Kinetic constants, $\text{min}^{-1}$	Relative coefficients, $R^2$
$\text{TiO}_2$ powder	$K_1 = 0.0127$	0.9913
$\text{TiO}_2$ nanotubes	$K_2 = 0.0171$	0.9959
$\text{TiO}_{2(0.2\text{M H}_2\text{SO}_4)}$ nanotubes	$K_3 = 0.0364$	0.9117
$\text{TiO}_{2(1.0\text{M H}_2\text{SO}_4)}$ nanotubes	$K_4 = 0.0535$	0.9336

### 3 Conclusions

$\text{TiO}_2$  nanotubes were fabricated via NaOH treatment at 150 °C for 20 h. Numerous fiberlike nanotubes grew from a micro-size  $\text{TiO}_2$  particle. The tube is open and hollow. Its diameter of nanotube was about 12 nm. The results from photocatalytic experiment of acid orange II indicated that photocatalytic activity of  $\text{TiO}_2$  nanotube is higher than that of

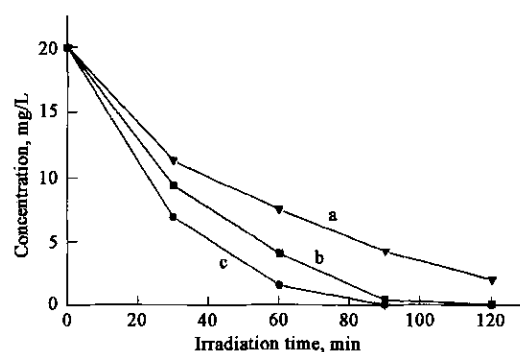


Fig. 6 Photocatalytic degradation of acid orange II in the presence of  $\text{TiO}_2$  nanotube(a),  $\text{TiO}_{2(0.2\text{M H}_2\text{SO}_4)}$  nanotubes(b) and  $\text{TiO}_{2(1.0\text{M H}_2\text{SO}_4)}$  nanotubes (c)

$\text{TiO}_2$  powder, that of  $\text{TiO}_{2(1.0\text{M H}_2\text{SO}_4)}$  nanotubes is the best, and that of  $\text{TiO}_{2(0.2\text{M H}_2\text{SO}_4)}$  nanotubes is medium. This was attributed to the fact that  $\text{TiO}_2$  nanotubes treated with  $\text{H}_2\text{SO}_4$  was composed of smaller particles and had higher specific surface area. Furthermore, the smaller  $\text{TiO}_2$  particles was beneficial to transfer and separation of photo-generated electrons and holes in the inner of and on the surface of  $\text{TiO}_2$  particle and reduced the recombination of photo-generated electrons and holes.

### References:

- Adachi M, Murata Y, Harada M *et al.*, 2000. Formation of titania nanotubes with high photo-catalytic activity[J]. *Chem Lett*, 8: 942.
- Anpo M, Shima T, Kodama S *et al.*, 1987. Photocatalytic hydrogenation of propyne with water on small-particle titania: size quantization effects and reaction intermediates[J]. *J Phys Chem*, 91: 4305—4310.
- Caruso R A, Schattk J H, Greiner A, 2001. Titanium dioxide tubes from sol-gel coating of electrospun polymer fibers[J]. *Advanced Materials*, 13: 1577—1579.
- Du G H, Chen Q, Che R C *et al.*, 2001. Preparation and structure analysis of titanium oxide nanotubes[J]. *Appl Phys Lett*, 79: 3702—3704.
- Duonghong D, Borgarello E, Gratzel M, 1981. Dynamics of light-induced water cleavage in colloidal systems[J]. *J Am Chem Soc*, 103:4685—4690
- Hoyer P, 1996. Formation of a titanium dioxide nanotube array[J]. *Langmuir*, 12: 1411—1413.
- Imai H, Takei Y, Shimizu K *et al.*, 1999. Direct preparation of anatase  $\text{TiO}_2$  nanotubes in porous alumina membranes[J]. *J Mater Chem*, 9: 2971—2972.
- Kato K, Tsuzuki A, Taoda H *et al.*, 1994. Photoelectrochemical characterization of nanocrystalline  $\text{TiO}_2$  films on titanium substrates[J]. *J Mater Sci*, 29: 5911—5919.
- Kasuga T, Hiramatsu M, Hoson A *et al.*, 1999. Titania nanotubes prepared by chemical processing[J]. *Adv Mater*, 11: 1307—1311.
- Kasuga T, Hiramatsu M, Hoson A *et al.*, 1998. Formation of titanium oxide nanotube[J]. *Langmuir*, 14: 3160—3163.
- Linsebigler A L, Lu G, Yates J T. 1995. Photocatalysis on  $\text{TiO}_2$  surfaces: principles, mechanisms and selected results[J]. *Chem Rev*, 95: 735—758.
- Ma D L, Linda S S, Richard W S L *et al.*, 2003. Preparation and structure investigation of nanoparticle-assembled titanium dioxide microtubes[J]. *Appl Phys Lett*, 83: 1839—1841.
- Michailowski A, AlMawlawi D, Cheng G S *et al.*, 2001. Highly regular anatase nanotube arrays fabricated in porous anodic templates[J]. *Chem Phys Lett*, 349: 1—5.
- Sene J J, Zeltner W A, Anderson M A, 2003. Fundamental photoelectrocatalytic and electrophoretic mobility studies of  $\text{TiO}_2$  and V-doped  $\text{TiO}_2$  thin-film electrode materials[J]. *J Phys Chem B*, 10: 1597—1603.
- Zhang Q, Cao L, Sun J *et al.*, 2002. Preparation of long  $\text{TiO}_2$  nanotubes from ultrafine rutile nanocrystals[J]. *Chem Lett*, 2: 226—228.
- Zhu Y, Li H, Koltypin Y *et al.*, 2001. Sonochemical synthesis of titania whiskers and nanotubes[J]. *Chem Commun*, 24: 2616—2617.